OSU Oregon State UNIVERSITY

Open Access Articles

Amorphous In-Ga-Zn-O thin-film transistors fabricated by microcontact printing

The Faculty of Oregon State University has made this article openly available.
Please share how this access benefits you. Your story matters.

Citation	Du, X., Frederick, R. T., Li, Y., Zhou, Z., Stickle, W. F., & Herman, G. S. (2015). Amorphous In-Ga-Zn-O thin-film transistors fabricated by microcontact printing. Journal of Vacuum Science & Technology B, 33(5), 052208. doi:10.1116/1.4929984
DOI	10.1116/1.4929984
Publisher	American Institute of Physics
Version	Version of Record
Terms of Use	http://cdss.library.oregonstate.edu/sa-termsofuse

Oregon State UNIVERSITY OSU

CrossMark click for updates

Amorphous In-Ga-Zn-O thin-film transistors fabricated by microcontact printing

Xiaosong Du[a] and Ryan T. Frederick
School of Chemical, Biological, and Environmental Engineering, Oregon State University, Corvallis, Oregon 97331

Yajuan Li
School of Chemical, Biological, and Environmental Engineering, Oregon State University, Corvallis, Oregon 97331 and College of Science, Civil Aviation University of China, Tianjin 300300, China

Zheng Zhou
School of Chemical, Biological, and Environmental Engineering, Oregon State University, Corvallis, Oregon 97331

William F. Stickle
Hewlett Packard Company, Corvallis, Oregon 97330

Gregory S. Herman[b]
School of Chemical, Biological, and Environmental Engineering, Oregon State University, Corvallis, Oregon 97331

(Received 3 July 2015; accepted 21 August 2015; published 3 September 2015)

The authors present a facile, low-cost methodology to fabricate high-performance In-Ga-Zn-O (IGZO) bottom contact, bottom gate thin-film transistors (TFTs) by soft lithography. The IGZO channel and indium tin oxide (ITO) source and drain were patterned using microcontact printing of an octadecylphosphonic acid self-assembled monolayer (SAM). A polymer stamp was used for the pattern transfer of the SAMs, which were then used as a chemical protection layer during wet etching. Excellent pattern transfer was obtained with good resolution and sharp step profiles. X-ray photoelectron spectroscopy indicated that the microcontact printed SAMs can be effectively removed from the ITO source/drain surfaces, allowing a high-quality interface to the IGZO channel for good device performance. Scanning electron microscopy cross-sections of the devices indicate a smooth and defect-free transition regions between the source/drain and semiconductor regions. The fabricated TFTs have negligible gate-leakage currents, high average electron mobilities of 10.2 cm^2/Vs, and excellent on-off ratios of 2.1×10^8. These results may provide new methodologies for low-cost and large-area integration of IGZO-TFTs for a range of applications including flexible and transparent displays. © *2015 American Vacuum Society*. [http://dx.doi.org/10.1116/1.4929984]

I. INTRODUCTION

Indium gallium zinc oxide (IGZO) has gained considerable attention as an oxide semiconductor for thin-film transistors (TFTs) over the past decade due to its low cost, ease in fabrication of TFTs with good performance, and for potential applications, including flexible and transparent electronic devices.[1,2] IGZO TFTs have relatively high average electron mobilities ($\mu_{avg} > 10\,cm^2/Vs$) despite being amorphous, and have been widely studied for use in a variety of applications, including flat panel displays,[1,3,4] gas detection,[5] temperature,[6] and light sensing.[7] High-performance IGZO-TFTs are also compatible with low temperature processing, which is necessary for flexible electronics on polymeric substrates.[1,8] IGZO-TFTs have recently replaced amorphous silicon TFT technologies for several display applications.[3,9] For display applications, the reliability of IGZO-TFTs is very important and bias and bias-illumination stress measurements have previously been performed on IGZO devices.[10,11] These results indicate that care must be taken in optimizing processes to obtain IGZO-TFTs with high stability.

Solution-based printing of IGZO-TFTs have been demonstrated;[12,13] however, typically much better device performance (e.g., device to device uniformity, increased electron mobility and stability, reduced hysteresis, and high drain current on/off ratios) can be obtained using vacuum deposited films. The fabrication of TFTs from vacuum deposited films usually is performed using photolithography and etching for patterning, which is typically expensive.[4] Low-cost alternative patterning methods, such as soft lithography, may be of great benefit to large-scale manufacturing, especially for roll-to-roll processes.[14–16] Microcontact printing (μCP) is a soft lithography approach where self-assembled monolayers (SAMs) are transferred from a patterned stamp onto a surface, and the SAMs are used as resists to prevent chemical etching,[14] and as initiators or surface energy modulators to guide material deposition.[17] μCP has been shown to be a convenient, low-cost method to pattern transparent oxide films, including indium tin oxide (ITO) and indium zinc oxide, with minimum feature sizes $\sim 2\,\mu m$, which is below the critical dimensions required for displays.[18] Alkane phosphonic acid inks can be printed using μCP and have been

[a]Electronic mail: duxi@onid.oregonstate.edu
[b]Electronic mail: greg.herman@oregonstate.edu

Redistribution subject to AVS license or copyright; see http://scitation.aip.org/termsconditions. Download to IP: 128.193.162.224 On: Mon, 19 Oct 2015 18:43:56

found to chemisorb to metal oxide surfaces forming robust, dense protective layers that allow wet etching of only the unprotected regions.[19,20] Patterned ITO films are important for display applications since ITO has a low resistivity and high transmittance in the visible range,[21] and provides good electrical contact to IGZO.

For organic transistors, μCP has been used to pattern source and drain electrodes,[22,23] gate electrode seed layers,[24] ultrathin gate dielectrics,[25] and to control the structure and electronic properties of organic semiconductors.[26] Studies have indicated that μCP can be used to pattern a range of other semiconductor based materials for transistors, including organic–inorganic hybrid materials,[17,27] zinc oxide,[28] and many others. Recent studies have also shown that μCP can be used to selectively pattern cobalt source/drain (S/D) electrodes on IGZO during fabrication of TFTs.[29]

In this letter, we demonstrate the patterning of ITO source/drain and IGZO channel materials by μCP. The physical, chemical, and electrical properties of the thin films and IGZO-TFTs are investigated. These results indicate that low-cost manufacturing approaches proven to work in other transparent oxide materials allow the fabrication of high-performance TFTs based on the emerging a-IGZO TFT technology. The proposed methodology herein can be applied to a range of TFT technologies, and can potentially lead to continuous roll-to-roll processing of IGZO-TFTs under ambient conditions.

II. EXPERIMENT

A. Materials

Octadecylphosphonic acid (OPDA) was purchased from specific polymers. Tridecafluoro-1,1,2,2-tetrahydrooctyl-1-trichlorosilane (TFOCS) was purchased from UCT Specialties. The SU-8 photoresist was acquired from Microchem. IGZO and ITO targets have been purchased from AJA International Inc. and Kurt J. Lesker Inc., respectively. Sylgard 184 polydimethylsiloxane (PDMS) was obtained from Dow Corning. Milli-Q water was used in all sample preparation.

B. Fabrication of μCP stamp

An epoxy-based negative photoresist (SU-8) was spin-coated onto a clean silicon wafer.[44] The photomask was aligned in close contact with the wafer and an ultraviolet light source (model 100UV30S1, Karlsus, Inc.) with wavelength $\sim$360 nm was used to expose the photoresist. Developer solution was used to remove unexposed regions of SU-8 from the substrate. The remaining SU-8 pattern on the silicon wafer (the master) had a depth of approximately 20 μm as measured by profilometry (KLA-Tencor Alpha-Step 500). TFOCS was deposited as a monolayer on the master through siloxane bonding by placing the master in TFOCS vapor for 30 min. Liquid prepolymer *PDMS* with curing agent (5:1 weight ratio) was cast onto the master followed by degassing for 30 min in vacuum. The PDMS was cured in an oven at 70 °C for 7 h, and then, a fresh PDMS stamp with features opposite to the master was fabricated by peeling the PDMS stamp from the master substrate.

C. Device fabrication and electrical measurement

μCP TFT test structures were fabricated as follows. A heavily p-doped Si substrate was used as the gate with thermally grown SiO_2 (100 nm) as the gate dielectric. ITO films (160 nm thick, measured by ellipsometry) were deposited using RF magnetron sputter deposition with a 3 in. ITO target (composition: In_2O_3:SnO_2 = 90:10 wt. %), 120 W RF power, $\sim$4 mTorr chamber pressure, and 20 sccm flow rate of Ar. Before patterning by microcontact printing, the ITO films were cleaned by UV-ozone treatment for 15 min (PSD standard, Novascan). An ODPA SAM was formed on the PDMS stamp by immersion in 5 mM ODPA/isopropyl alcohol for 5 min. The SAM was transferred from the PDMS stamp to oxide film after a $\sim$60 s contact time. After SAM transfer the unprotected ITO was etched at a rate of 10 nm/min in 50 mM aqueous oxalic acid solution, with mild agitation. To remove the ODPA ink, the ITO surface was rinsed with 2-propanol followed by oxygen plasma cleaning for 5 min at 50 W (PE-100, Plasma Etch, Inc.). The ITO films were then annealed at 300 °C for 1 h to increase their resistance to the oxalic acid etch, increase their electrical conductivity, and improve their transparency.

Amorphous IGZO films ($\sim$50 nm thick) were deposited by sputter deposition with a 3 in. IGZO sputter target (molar composition: In_2O_3:Ga_2O_3:ZnO), 100 W RF power, $\sim$4 mTorr chamber pressure, and 20 sccm flow rate with a 1:19 (O_2:Ar) ratio. IGZO active layers were patterned subsequently by microcontact printing, using the same procedures as the ITO films with an etch rate of 40 nm/min in 50 mM aqueous oxalic acid solution. The ODPA ink printed on IGZO surface was removed by 2-propanol rinsing and oxygen plasma treatment. The fabricated TFTs were annealed in air at 300 °C to improve the device performance, and the resulting TFTs had a width/length (W/L) ratio of 1000/100 μm.

For comparison, IGZO-TFT test structures were also fabricated by shadow mask patterning.[45] We use the same heavily p-doped Si substrates as the gate, and thermally grown SiO_2 (100 nm) as the gate dielectric. Source/drain electrodes were patterned using a shadow mask during ITO deposition ($\sim$160 nm thick) giving a W/L ratio of 1000/100 μm. IGZO active layers ($\sim$50 nm thick) were patterned using a shadow mask during deposition, and the films were subsequently annealed in air to 300 °C.

All IGZO-TFT electric measurements were performed in the dark at room temperature in air using an Agilent 4155C precision semiconductor parameter analyzer. Drain current vs drain voltage (I_D-V_D) output curves were measured for several gate voltages (V_G = 2, 4, 6, 8, and 10 V) and with a V_D sweep step size of 0.2 V. Forward (low voltage to high voltage) and backward (high voltage to low voltage) sweep drain-to-source current vs gate voltage (I_D-V_G) transfer curves were measured with the drain voltage (V_D) set to 1 V with a V_G sweep step size of 0.2 V.

D. X-ray photoelectron spectroscopy

X-ray photoelectron spectroscopy (XPS) measurements were performed with a PHI Quantera Scanning ESCA

Redistribution subject to AVS license or copyright; see http://scitation.aip.org/termsconditions. Download to IP: 128.193.162.224 On: Mon, 19 Oct 2015 18:43:56

system using monochromatized Al Kα radiation (photon energy of 1486.6 eV) with a 200 μm spot size. The energy scale of the spectrometer was calibrated to Au $4f_{7/2}$ at 84.0 eV and Cu $2p_{3/2}$ at 932.7 eV. Charge compensation was accomplished using a combination of low energy ion and electron beams coincident on the sample. The data were quantified using instrument standard relative sensitivity factors corrected for the transmission function of the analyzer. The data were acquired with a 45° emission angle and an electron analyzer pass energy of 69 eV. The XPS data were fit using CASAXPS, where the most intense peak in the spectrum was used to define the core-level full-width-half-maximum (FWHM) and Gaussian–Lorentzian mixing. A linear background was used to fit all spectra. The binding energies were charge corrected to the C 1s aliphatic carbon peak at 284.6 eV.

E. Scanning electron microscopy

Samples were prepared as cross-sections via focused ion-beam (FIB) using an FEI 3D DualBeam scanning electron microscope. Approximately 30 nm of amorphous carbon, 10 nm of chromium and 1 μm Pt were thermally evaporated on the sample to serve as a protective layer stack prior to the cross section process. Thin film cuts were performed by FIB using a Ga beam at 30 kV with a 3 nA beam current to form cross sections, which were then followed with 50 pA beam current to clean the cross-sections. Images were collected in a FEI 3D DualBeam at 10.0 kV and a working distance of 9.9 mm.

III. RESULTS AND DISCUSSION

A schematic of the IGZO-TFT structure is shown in Fig. 1(a), while an optical image of a μCP fabricated IGZO-TFT is shown in Fig. 1(b). A bottom contact, bottom gate structure was used due to the relative etch selectivity in oxalic acid (i.e., much higher etch rate for IGZO compared to ITO). The prepared master (epoxy-based negative photoresist SU-8 pattern on Si) shown in Figs. S1(A) and S1(B)[30] has well-resolved features that are transferred to the PDMS stamp pattern shown in Figs. S1(C) and S1(D).[30] Upon close inspection, even the ridges on the PDMS stamp were replicates of the grooves in the SU-8 master. Phosphonic acid has been used to tune the surface

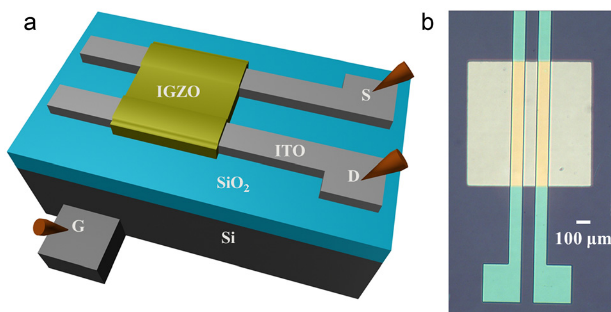

FIG. 1. (Color online) (a) Schematic illustration and (b) optical image of IGZO TFT structure. The patterned source and drain (S/D) define the width/length (W/L) ratio of 1000/100 μm.

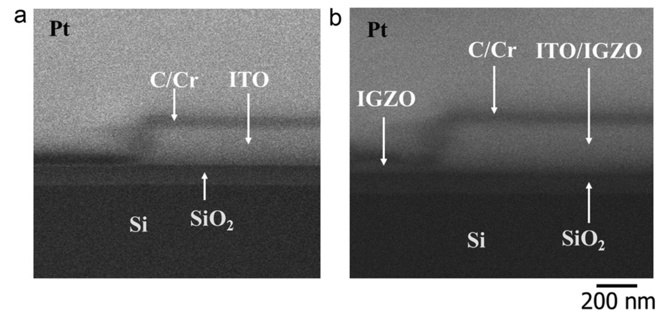

FIG. 2. SEM cross-section images of the edge (a) between ITO and substrate and (b) between IGZO/ITO and IGZO.

properties of metal oxide films;[18,20,31–33] and for these studies, we used ODPA ink as the protective layers on top of the blanket ITO film. We found that the μCP ODPA transferred ink was continuous and provided excellent etch resistance to oxalic acid. The patterned ITO is shown in Fig. 1(b) and did not show any resolution loss or visible defects. After the removal of ODPA using an O_2 plasma, the sample was annealed at 300 °C for 1 h in air. The annealing was used to increase the crystallinity of the ITO films, which significantly reduced the etch rate to less than 1 nm/min. This ensures the ITO pattern will be preserved during the IGZO etching step. IGZO deposition and μCP also yielded good quality patterning of the channel material, which is essential to uniform device performance of TFTs.

Scanning electron microscopy (SEM) was used to characterize the step edge profiles of patterned ITO source and drain as shown in Fig. 2. Figure 2(a) shows the ITO step edge between ITO source/drain and the SiO_2 dielectric layer. The ITO layer in this region has a smooth, defect free slope

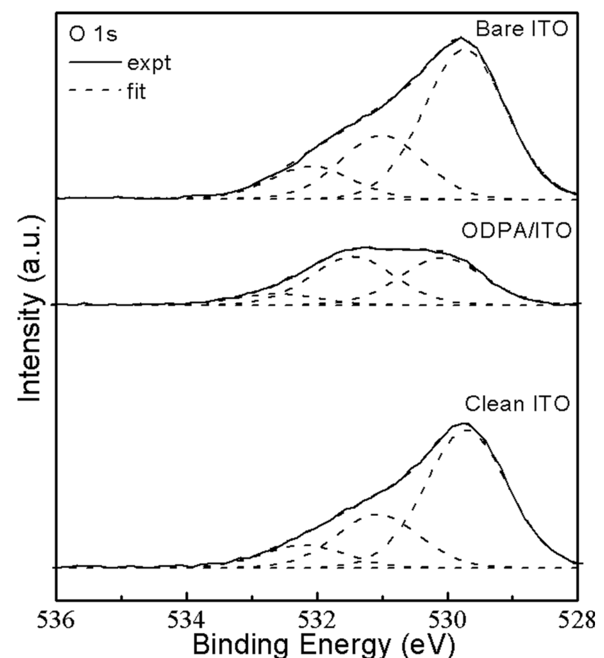

FIG. 3. O 1s XPS data obtained from blanket ITO films (upper), ITO films that have printed ODPA ink (middle), and ITO films after O_2 plasma cleaning (lower).

Redistribution subject to AVS license or copyright; see http://scitation.aip.org/termsconditions. Download to IP: 128.193.162.224 On: Mon, 19 Oct 2015 18:43:56

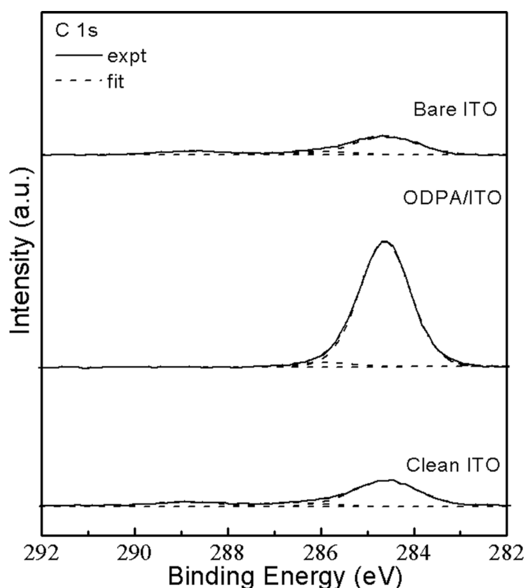

FIG. 4. C 1s XPS data obtained from blanket ITO films (upper), ITO films that have printed ODPA ink (middle), and ITO films after O_2 plasma cleaning (lower).

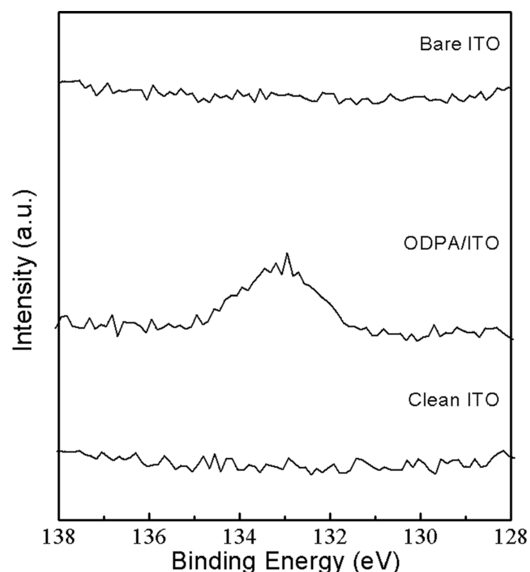

FIG. 5. P 2p XPS data obtained from blanket ITO films (upper), ITO films that have printed ODPA ink (middle), and ITO films after O_2 plasma cleaning (lower).

with a width <100 nm from the region with no ITO to the region with 160 nm thick ITO. Figure 2(b) shows the region transitioning from the IGZO layer to the region that contains both IGZO and ITO. A similar width (<100 nm) was observed for the transition from IGZO to the ITO/IGZO region that has a combined thickness 210 nm.

XPS was used to investigate the adsorption of ODPA molecules to the metal oxide surfaces. In the upper portion of Fig. 3 we show O 1s XPS data for a blanket ITO film, the middle portion shows data from printed ODPA on ITO film, and the lower portion shows clean ITO film after the oxygen plasma treatment for ODPA removal. To fit the O 1s core level spectrum for the ITO film, it is necessary to use three components, similar to what has been done previously.[34–38] The main O(1s) peak at $E_b = 529.7$ eV is associated with lattice oxygen ions. A shoulder which corresponds to a peak at $E_b = 531.0$ eV is attributed to surface hydroxyl groups. The high-energy O 1s peak at $E_b = 532.0$ eV is due to other surface contaminates. After printing ODPA, as shown in the middle portion of Fig. 3, a new peak at $E_b = 531.5$ eV appears, and corresponds to P–O–In/P-O-Sn and P=O bonds.[39] Additionally, a decrease in the peak intensity of the peaks associated with lattice oxygen ions was observed due to the attenuation of photoelectrons from the bulk film through the ODPA layer. After oxygen plasma treatment, as shown in the lower portion of Fig. 3, the O 1s spectrum recovers to the original bare ITO surface.

In the upper portion of Fig. 4, we show C 1s spectra for a blanket ITO film. The C 1s spectra had three fairly well-separated peaks with the lower energy peak having an energy of $E_b = 284.6$ eV, which is assigned to aliphatic carbon (C–C or C–H bonds), and the two higher energy peaks at $E_b = 286.1$ and 288.7 eV are assigned to C–O and O–C=O groups on the surface, respectively.[40,41] As shown in the middle portion of Fig. 4, most of the C 1s intensity from the ITO sample with ODPA comes from aliphatic carbons in the ODPA molecules, and a higher energy peak at $E_b = 285.9$ due to $-CH_2-$ bonded to the phosphonic acid group. As shown in

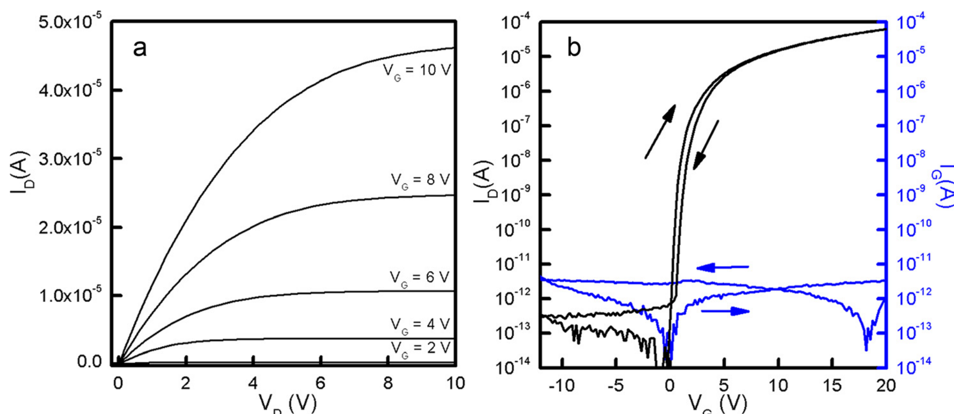

FIG. 6. (Color online) Device performance of IGZO-TFT fabricated by microcontact printing. (a) Output characteristics and (b) transfer characteristics (V_D = 1 V, W/L ratio of 1000/100 μm).

Redistribution subject to AVS license or copyright; see http://scitation.aip.org/termsconditions. Download to IP: 128.193.162.224 On: Mon, 19 Oct 2015 18:43:56

the lower portion of Fig. 4, the oxygen plasma treatment is effective in removal of the carbon associated with the OPDA.

In Fig. 5, the P 2p spectra are shown for the samples discussed above, where the upper portion is for a blanket ITO film, the middle portion is the data from printed ODPA on ITO film, and the lower portion is the clean ITO film after the oxygen plasma treatment for ODPA removal. A core-level peak associated to P 2p electrons is present only for the ODPA-printed samples. The successful removal of the ODPA ink was confirmed by removal of the P 2p peaks in the lower portion of Fig. 5. Similar XPS data were obtained for the IGZO films and are provided in the supplementary material.[30] Peak positions and area ratios were quantitatively summarized and are provided in Table SI.[30]

The electric performance of the fabricated TFT device has been measured and the drain current (I_D)-drain voltage (V_D) characteristics at various gate voltages (V_G) are shown in Fig. 6(a). Typical accumulation mode n-channel transistor behavior was obtained, where a linear regime (the field-effect current modulation) and a saturation regime at high V_G were both observed.[42] No current crowding was observed for these devices suggesting good S/D contact to the IGZO film. A representative transfer characteristic of the IGZO-TFTs was obtained by sweeping I_D vs V_G with a constant V_D and is shown in Fig. 6(b). In Table I, we provide the average electron mobility (μ_{avg}), turn-on voltage (V_{ON}), drain current on-to-off ratio (I_{ON}/I_{OFF}), and hysteresis (difference in the V_G up and down sweeps in the I_D-V_G data). IGZO-TFTs fabricated using shadow masks were measured for comparison. μ_{avg} can be obtained from the following equation:

$$\mu_{avg} = \frac{G_{CH}}{\frac{W}{L} C_{ins}(V_G - V_{ON})},$$

where G_{CH} and C_{ins} is the channel conductance and the gate insulator capacitance per unit area, respectively.[43] The TFTs did not have significant hysteresis between the up and down sweeps, suggesting traps have the ability to stay in equilibrium with the sweep rate of $V_G = 0.2$ V/s. A high I_{ON}/I_{OFF} ratio $\sim 10^8$ and high $\mu_{avg} > 10\,cm^2/Vs$ were obtained, while the gate leakage currents (I_G) were typically $<nA/cm^2$. IGZO-TFTs patterned using μCP and shadow mask based methods show very similar performance, which indicates that μCP patterned materials are robust for device integration, have good semiconductor/source and drain interfaces, and have high-quality dielectric/channel interface.

TABLE I. Average mobility, turn on voltage, drain current on-to-off ratio, and hysteresis for IGZO TFTs fabricated by μCP and shadow mask patterning ($V_D = 1$ V).

IGZO-TFT	μ_{avg} (cm^2/Vs)	V_{on} (V)	I_{on}/I_{off}	Hysteresis (V)
μCP	10.2	0.1	2.1×10^8	0.6
Shadow mask	9.2	−0.5	1.2×10^8	0.9

IV. SUMMARY AND CONCLUSIONS

In summary, high-performance IGZO-TFTs were successfully fabricated using microcontact printing to pattern sputter deposited IGZO and ITO layers. ITO S/D and IGZO channel were patterned without visible defects using a PDMS stamp to transfer ODPA, followed by oxalic acid etching. The printed pattern provided good replication of the PDMS stamp. SEM cross-section and imaging further indicate the presence of well-defined step edges marked by a smooth and defect-free slope from one layer to another. XPS indicated complete removal of ODPA ink from the metal oxide surfaces after O_2 plasma treatment, and provides clean interfaces for device integration. The IGZO-TFTs had excellent electrical characteristics, indicating that a convenient and low-cost route can be used to fabricate high performance IGZO-TFTs.

ACKNOWLEDGMENTS

X.D. acknowledges funding from the Juvenile Diabetes Research Foundation (3-PDF-2014-113-A-N). R.T.F. and G.S.H. acknowledge support from the Center for Sustainable Materials Chemistry, which is supported by the U.S. National Science Foundation under Grant CHE-1102637. Y.L. acknowledges the support of China Scholarship Council and the Science Foundation of Civil Aviation University of China (3122013k006). The authors thank Peter Eschbach and Josh Motley (Oregon State University) for assistance with the electron microscopy and schematic drawings, respectively.

[1] K. Nomura, H. Ohta, A. Takagi, T. Kamiya, M. Hirano, and H. Hosono, Nature **432**, 488 (2004).
[2] L. Xifeng, X. Enlong, S. Jifeng, L. Chunya, and Z. Jianhua, J. Vac. Sci. Technol. A **31**, 031505 (2013).
[3] T. Kamiya, K. Nomura, and H. Hosono, Sci. Technol. Adv. Mater. **11**, 044305 (2010).
[4] E. Fortunato, P. Barquinha, and R. Martins, Adv. Mater. **24**, 2945 (2012).
[5] H.-W. Zan, C.-H. Li, C.-C. Yeh, M.-Z. Dai, H.-F. Meng, and C.-C. Tsai, Appl. Phys. Lett. **98**, 253503 (2011).
[6] J. Hoon, K. Chung Sik, C. Sung Wook, P. Kwon Shik, L. Sang Gul, H. Yong Min, and J. Jin, IEEE Electron Device Lett. **34**, 1569 (2013).
[7] H.-W. Zan, W.-T. Chen, H.-W. Hsueh, S.-C. Kao, M.-C. Ku, C.-C. Tsai, and H.-F. Meng, Appl. Phys. Lett. **97**, 203506 (2010).
[8] J.-S. Park *et al.*, Appl. Phys. Lett. **95**, 013503 (2009).
[9] J. F. Wager, D. A. Keszler, and R. E. Presley, *Transparent Electronics* (Springer, Berlin, 2008).
[10] A. Suresh and J. F. Muth, Appl. Phys. Lett. **92**, 033502 (2008).
[11] R. N. P. Vemuri, M. R. Hasin, and T. L. Alford, J. Vac. Sci. Technol. A **32**, 021101 (2014).
[12] S. Jeong *et al.*, J. Mater. Chem. C **1**, 4236 (2013).
[13] K. Everaerts, L. Zeng, J. W. Hennek, D. I. Camacho, D. Jariwala, M. J. Bedzyk, M. C. Hersam, and T. J. Marks, ACS Appl. Mater. Interfaces **5**, 11884 (2013).
[14] J. C. Love, L. A. Estroff, J. K. Kriebel, R. G. Nuzzo, and G. M. Whitesides, Chem. Rev. **105**, 1103 (2005).
[15] Y. Xia, E. Kim, X.-M. Zhao, J. A. Rogers, M. Prentiss, and G. M. Whitesides, Science **273**, 347 (1996).
[16] X. Du *et al.*, ECS J. Solid State Sci. Technol. **4**, P3069 (2015).
[17] C. R. Kagan, T. L. Breen, and L. L. Kosbar, Appl. Phys. Lett. **79**, 3536 (2001).
[18] T. L. Breen, P. M. Fryer, R. W. Nunes, and M. E. Rothwell, Langmuir **18**, 194 (2002).
[19] P. J. Hotchkiss, S. C. Jones, S. A. Paniagua, A. Sharma, B. Kippelen, N. R. Armstrong, and S. R. Marder, Acc. Chem. Res. **45**, 337 (2012).

Redistribution subject to AVS license or copyright; see http://scitation.aip.org/termsconditions. Download to IP: 128.193.162.224 On: Mon, 19 Oct 2015 18:43:56

[20]P. J. Hotchkiss, M. Malicki, A. J. Giordano, N. R. Armstrong, and S. R. Marder, J. Mater. Chem. **21**, 3107 (2011).
[21]L.-J. Meng and M. P. dos Santos, Thin Solid Films **322**, 56 (1998).
[22]J. Tate *et al.*, Langmuir **16**, 6054 (2000).
[23]D. Kim and D.-Y. Khang, Polymer **55**, 2491 (2014).
[24]U. Zschieschang, H. Klauk, M. Halik, G. Schmid, and C. Dehm, Adv. Mater. **15**, 1147 (2003).
[25]U. Zschieschang, M. Halik, and H. Klauk, Langmuir **24**, 1665 (2008).
[26]T. Kushida, T. Nagase, and H. Naito, Org. Electron. **11**, 1323 (2010).
[27]J. Mehlich, Y. Miyata, H. Shinohara, and B. J. Ravoo, Small **8**, 2258 (2012).
[28]T. V. Richter, F. Stelzl, J. Schulz-Gericke, B. Kerscher, U. Wurfel, M. Niggemann, and S. Ludwigs, J. Mater. Chem. **20**, 874 (2010).
[29]Y.-J. Cho, H. Kim, K.-Y. Park, J. Lee, S. M. Bobade, F.-C. Wu, and D.-K. Choi, J. Nanosci. Nanotechnol. **11**, 787 (2011).
[30]See supplementary material at http://dx.doi.org/10.1116/1.4929984 for optical microscopy images of device fabrication, O 1s, C 1s, P 2p XPS data obtained from blanket IGZO films, and XPS binding energies and peak areas.
[31]X. Du, B. T. Flynn, J. R. Motley, W. F. Stickle, H. Bluhm, and G. S. Herman, ECS J. Solid State Sci. Technol. **3**, Q3045 (2014).
[32]P. B. Paramonov, S. A. Paniagua, P. J. Hotchkiss, S. C. Jones, N. R. Armstrong, S. R. Marder, and J.-L. Brédas, Chem. Mater. **20**, 5131 (2008).
[33]X. Du, Q. Li, H. Su, and J. Yang, Phys. Rev. B **74**, 233201 (2006).
[34]Y.-C. Huang, P.-Y. Yang, H.-Y. Huang, S.-J. Wang, and H.-C. Cheng, J. Nanosci. Nanotechnol. **12**, 5625 (2012).
[35]N. Thi Thu Thuy, O. Renault, B. Aventurier, G. Rodriguez, J. P. Barnes, and F. Templier, J. Disp. Technol. **9**, 770 (2013).
[36]M. J. Lee, S. J. Kang, J. Y. Baik, K.-j. Kim, H.-D. Kim, H.-J. Shin, J. Chung, J. Lee, and J. Lee, J. Appl. Phys. **108**, 024507 (2010).
[37]K. Nomura, T. Kamiya, E. Ikenaga, H. Yanagi, K. Kobayashi, and H. Hosono, J. Appl. Phys. **109**, 073726 (2011).
[38]N. Oka, T. Aoi, R. Hayashi, H. Kumomi, and Y. Shigesato, Appl. Phys. Express **5**, 075802 (2012).
[39]C. L. Perkins, J. Phys. Chem. C **113**, 18276 (2009).
[40]X. Deng, A. Verdaguer, T. Herranz, C. Weis, H. Bluhm, and M. Salmeron, Langmuir **24**, 9474 (2008).
[41]Y. Xie, X. Zhao, Y. Chen, Q. Zhao, and Q. Yuan, J. Solid State Chem. **180**, 3576 (2007).
[42]J. T. Anderson, C. L. Munsee, C. M. Hung, T. M. Phung, G. S. Herman, D. C. Johnson, J. F. Wager, and D. A. Keszler, Adv. Funct. Mater. **17**, 2117 (2007).
[43]R. L. Hoffman, J. Appl. Phys. **95**, 5813 (2004).
[44]D. Song, B. Song, H. Hu, X. Du, and Z. Ma, Appl. Thermal Eng. **85**, 356 (2015).
[45]D. Song, B. Song, H. Hu, X. Du, and F. Zhou, Phys. Chem. Chem. Phys. **17**, 13800 (2015).

Redistribution subject to AVS license or copyright; see http://scitation.aip.org/termsconditions. Download to IP: 128.193.162.224 On: Mon, 19 Oct 2015 18:43:56